

Investigation of time-reversed ultrasonic waves focusing in multilayered media

G. Butėnas, R. Kažys

Prof. K. Baršauskas Ultrasound Institute, Kaunas University of Technology

Studentų str. 50, Kaunas, Lithuania, tel. (+370 699 23373)

E-mail: gintas_butenas@yahoo.com

Abstract

In the paper we investigate the time-reversal approach application for non-destructive evaluation of layered structures and it is shown, that the time-reversal mirrors (TRM) can be used for detection of scattering sources in layered media and the time-reverted waves successfully pass through layer-stacking zones and refocuses to the initial source. The investigations were performed for two cases: 2-layered structure (liquid-solid) and 3-layered structure (liquid-solid-liquid). The results show that multiple reflections caused by different structure layers and boundaries were eliminated by the TRM. Wave energy does not dissipate after mode conversion at liquid-solid interfaces, but is redirected to waves which coincide in some arbitrary time instant. Numerical modeling was performed by finite element method using the commercially available software ABAQUS/Explicit.

Keywords: layered, time-reversal, focusing

Introduction

Nowadays the multilayered plates are the common construction materials in aerospace, marine craft and petroleum industry [12]. These structures offer many advantages in comparison to alloys, especially high strength and stiffness, excellent fatigue properties and corrosion resistance. Non-destructive testing of these materials is important research object, influenced by significant increment of crashed materials and defects emerged in a manufacturing process or during structure exploitation time. Very often the inspections during the operation can be difficult and maintenance complicated or impossible.

Cracks in composite laminated plates can be detected and characterized by conventional ultrasonic techniques, although reliable results are more difficult to obtain than for traditional materials, such as metals, that are homogeneous. Diameters of the individual fibers in fiber-reinforced composites are micrometers and the thicknesses of plies are of the order of the tenth of millimeter. It would not be productive to try to detection of cracks with the signals whose dominant wavelength is smaller than the ply thickness. Such signals would generate waves that have too much interference with inhomogeneity of the composite material, and they would be rapidly attenuated. In lower frequency range the signals whose dominant wavelength is of the order of the thickness of laminated plates, will propagate over longer distances since the wave will have less interference with the inhomogeneity of the material at such lower frequency signal. On the other hand, the lower frequency of the input signal the lower the spatial resolution is. Hence, it would be difficult to use very low wavelength signals whose dominant frequency is much longer than the plate thickness, even though they propagate long distances. Therefore, the signals with the central frequency whose dominant wavelength is about the thickness of the laminate are most preferred.

In this paper we investigate time-reversal method application to layered structures and it is shown, that the time reversal can be used for detection of a scattering source in the layered media and time-reverted waves

successfully propagate through layer-stacking zones and refocuses to the initial source. We investigated the time-reverted waves focusing in two cases:

1. 2-layered structure (liquid-solid);
2. 3-layered structure (liquid-solid-liquid).

Numerical modeling was performed by the finite element commercially available software ABAQUS/Explicit based on the explicit central-difference time integration scheme, which effectively can be used for modeling of wave propagation in such plates.

Time reversal approach to layered media

The time-reversal transformation of a wave propagation process can be usefully adapted for a wave excitation source characterization [1, 2, 3, 4]. The source of the wave can be not only an ultrasonic transducer, but also defect or interface between not matched layers in a multilayered structure. The time-reversal operation can be realized by the using time reversal mirrors (TRM) and a signal processing system. TRM is an array of transducers used for signal receiving and transmitting. The signal processing system is used only to record a wave as a function of the time and execute the time-reversal operation. After that the time reverted signal is sent back to the mirror and transmitted back to the medium. The time-reversed wavefield propagates through the medium and refocuses on the excitation point. Practically the time reversal approach can be implemented in two regimes – the through transmission (Fig. 1) and the pulse-echo (Fig. 2).

Time reversal through liquid-solid interface

The first stage of our investigation is wave propagation through a solid-liquid interface. Very often various liquids are used for transducer-structure matching purposes. Focusing behavior of the time-reversed wavefield through a liquid-solid interface may not work, because in the fluid propagate only pressure or longitudinal waves and in the solids propagate shear and longitudinal waves. It means that wave energy may be refocused or lost by mode conversion.

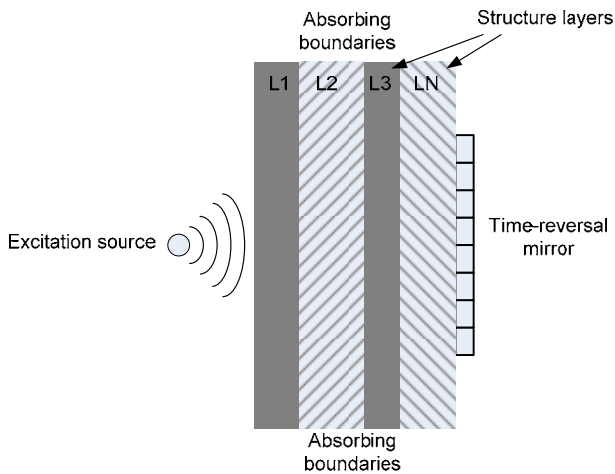


Fig. 1. Through-transmission time-reversal mirror principle

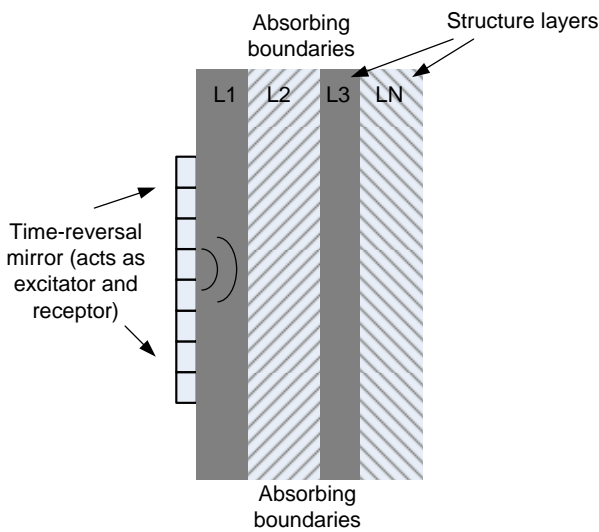


Fig. 2. Pulse-echo time-reversal mirror principle

The formulation of wave propagation in a solid can be expressed [5] as an acoustic displacement field $u(\mathbf{r}, t)$ in a solid [1]:

$$\rho_s \frac{\partial^2 \vec{u}}{\partial t^2} = (\lambda + 2\mu)(\nabla(\nabla \cdot \vec{u})) - \mu(\nabla \times (\nabla \times \vec{u})) \quad (1)$$

where ρ_s is the density of the solid, λ and μ are the Lamé's coefficients.

In the fluid an ultrasonic pressure [5] wave $P(r, t)$ satisfies the equation:

$$K(r) \frac{\partial^2 P}{\partial t^2} = \nabla \cdot \left(\frac{\nabla P}{\rho(r)} \right) \quad (2)$$

where $K(r)$ is the compressibility and ρ is the fluid density.

These equations contain only the second derivative with respect to the temporal variable which provides the strong property of being invariant in the time reversal procedure [5].

The boundary conditions at a solid/fluid interface require that the normal displacement and the normal stress would be continuous through the interface and that the

tangential shear stresses in the solid vanish on the interface. The tangential components of the displacement will be discontinuous through the interface.

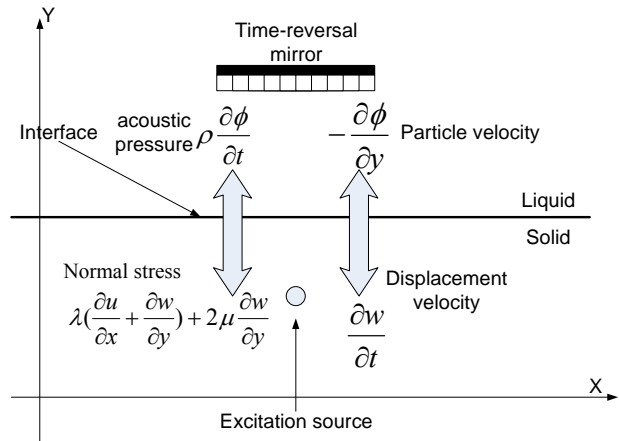


Fig. 3. Solid-liquid interface model

The time-reversal process modeling consists of three main steps:

1. Excitation of the initial wave in the solid.
2. Recording of the propagated sound pressure wave field $p(t)$ by all array elements.
3. Re-transmitting of the recorded and the time reversed wave field $p(T - t)$.

Numerical modeling

It is convenient to solve the equation system numerically by the finite element analysis (FEA), that the problem statement does not require big computational resources. As in the previous articles [2, 3] for a numerical modeling we constructed 2D FEA model based on the explicit central-difference time integration scheme implemented in the commercially available software ABAQUS/Explicit.

Elastic wave propagation analysis is performed by solving structural dynamic equation (ABAQUS/Explicit manual [11][10]):

$$[M]\{\ddot{U}\} + [C]\{\dot{U}\} + K\{U\} = \{F(t)\} \quad (3)$$

where $[M]$ is the mass, $[K]$ is the stiffness, $[C]=\alpha[M]$ is the proportional damping matrices; $\{F\}$ – external load vector, $\{U\}$ are the nodal displacement, velocity and acceleration vectors of the structure.

The time integration is performed by means of the central-difference integration scheme:

$$\{U_{t+\Delta t}\} = [\hat{M}]^{-1} \{F_t\} - ([K] - \frac{2}{\Delta t^2}[M])\{U_t\} - [\tilde{M}]\{U_{t-\Delta t}\}, \quad (4)$$

where:

$$[\hat{M}] = \frac{1}{\Delta t^2}[M] + \frac{1}{2\Delta t}[C] = \frac{1}{\Delta t^2}[M] + \frac{1}{2\Delta t}\alpha[M],$$

$$[\tilde{M}] = \frac{1}{\Delta t^2}[M] - \frac{1}{2\Delta t}[C] = \frac{1}{\Delta t^2}[M] - \frac{1}{2\Delta t}\alpha[M],$$

Δt is the time integration step.

Eq. 3 is arranged as:

$$\begin{aligned} \{U_{t+\Delta t}\} &= [\hat{M}]^{-1} \{F_t\} - [\hat{M}]^{-1} [K] \{U_t\} + \dots \\ &+ \frac{2}{\Delta t^2} [\tilde{M}]^{-1} \{U_t\} - [\hat{M}]^{-1} [\tilde{M}] \{U_{t-\Delta t}\} \end{aligned} \quad (5)$$

The fluid or in our case water we model as a solid, but with close to zero shear wave speed value. Regarding that consideration we calculate the abstract Young's and the Poisson's ratio modulus for water. Materials physical and mechanical data presented in Table 1 and the model mesh data are presented in Table 2.

Table 1. **Materials data**

Steel	
Density ρ	7800 [kg/m ³]
Young's Modulus, G	2.06x10 ¹¹ [N/m ²]
Poisson's Ratio, ν	0.29
Mechanical dimensions:	20x10mm
Water	
Density ρ	1000 [kg/m ³]
Young's Modulus, G	2.25x10 ⁹ [N/m ²]
Poisson's Ratio, ν	0.49
Mechanical dimensions:	20x10mm

Table 2. **FE data**

Number of nodes	161202
Number of elements	16000
Type of elements:	CPE4R – finite elements with reduced integration
Element linear size	50 μ m
Element per wavelength	15-30 elements (for shear and longitudinal wavelength)
Computational domain:	20x20mm

Table 3. **Transducers array data**

Linear array length [mm]:	12
Number of transducers	60
Transducers spacing	$\lambda/2$
Transducer length	$\lambda/3$ regular square

There was used CPE4R 4-node plane strain bilinear continuum element. Such an element provides the second-order interpolation, with a reduced integration and hourglass control (hour-glassing is a numerical phenomenon by which a zero-energy mode propagates through and spoils the solution – see ABAQUS Theory manual [11], Sec. 3.1.1, for more details). Each node has 2-degrees of freedom (plain strain assumption). In the mesh control that element is used when average strain is calculated, without the second-order accuracy and distortion control.

The transducers array is assumed to be a linear 1D array formed by regular line elements.

As an excitation source we used a point to which the concentrated load is applied. The load is the Gaussian modulated sine burst (three periods) with the of central frequency 3,5 MHz. The pulse duration is 0,4 μ s. This source is situated in the steel plate (assuming that the source can be any kind of defect) and geometrical coordinates are ($x = 10$ mm, $y = 5$ mm).

In forward and backward modeling we do not eliminate reflections from the walls, because they are linear and can be successfully removed by the TRM approach.

Modeling results

The snapshots of the solution are presented as a deformation field at different time instant. Fig. 4 shows snapshot of the initial wave excitation and propagation of longitudinal (fast) and shear (slow) waves in a steel plate. The generated waves propagate in the steel and attain to the solid-liquid boundary at 112 μ s (Fig. 5). After boundary only longitudinal wave propagate through the water (Fig. 6) and cross the time-reversal mirror, position of which is shown in Fig. 7. The signal is recorded by the mirror and retransmitted back to the medium. The retransmitted and back-propagated waves, interacts and form a wave-front, which is identical to the wave-front of the forward propagated wavefield (Fig. 8). At the time $t = 212$ μ s the instant waves refocus to the initial excitation point (Fig. 8). For this setup, the size of the focal spot is approximately equal to the size of the longest wavelength 2.5 mm. The lateral resolution of the method depends on the array aperture length, the distance between the array and the target, and the wavelength in a structure and is given by [13]:

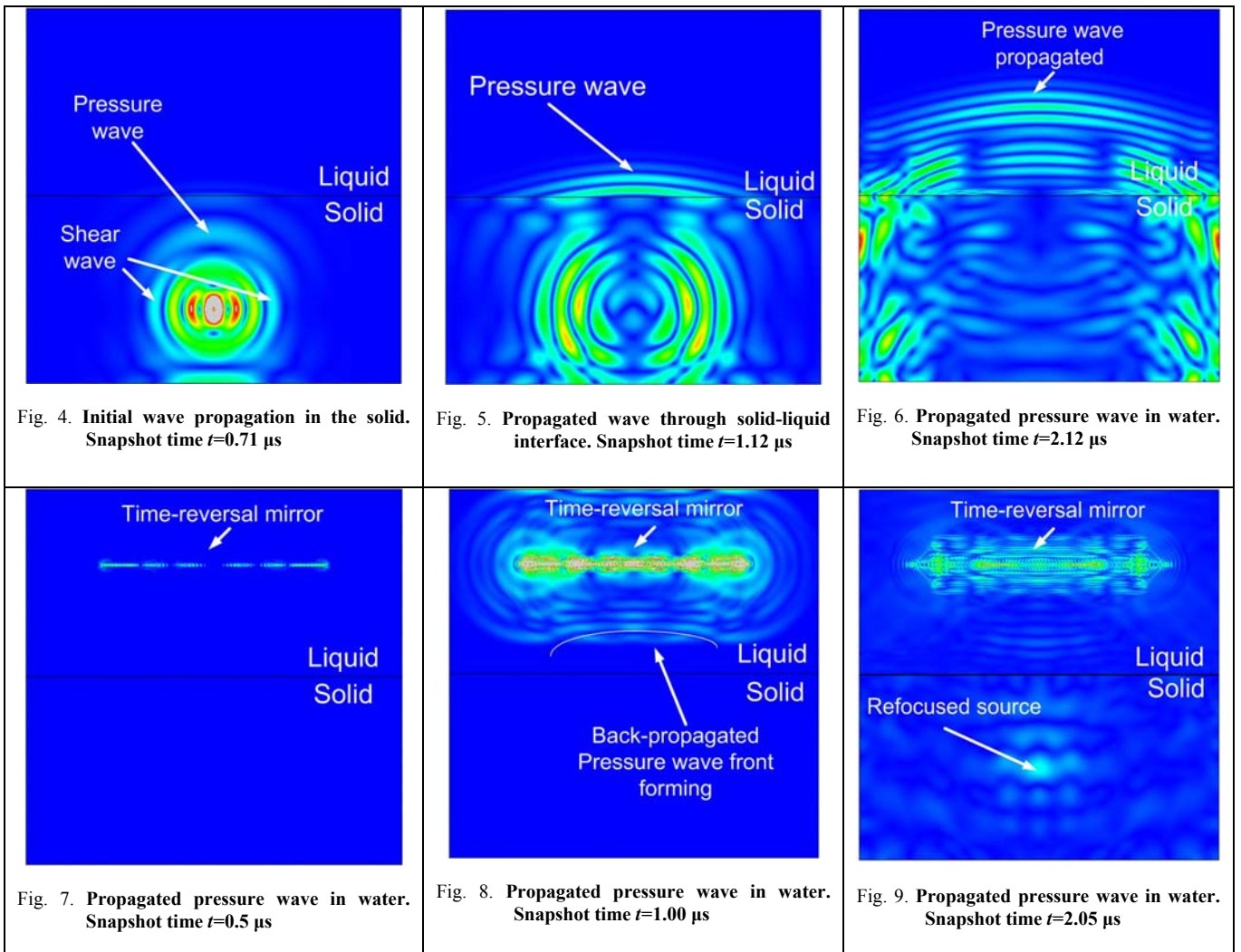
$$l = \frac{\lambda_{PS} L_S + \lambda_{PF} L_F}{d}; \quad (6)$$

where l is the lateral resolution, λ_{PS} is the wavelength of the pressure wave in the solid, L_S is the wave propagation distance in solid, λ_{PF} is the wavelength of the pressure wave in the fluid, L_F is the wave propagation distance in fluid, d is the aperture length of the linear transducers array.

Three-layered structure setup

In the next step, we modeled the situation that is closer to the real testing, where the structure is immersed in water. The process that we want to observe can be divided in to such periods:

1. Wave excitation at a point (x, y);
2. Propagation through the layer liquid-solid;
3. Propagation through the layer solid-liquid;
4. Signal capture by the transducers array (72 transducers, centered in the upper-water layer).
5. Signal reverting in the time domain;
6. Sending back;
7. Propagation through the layer liquid-solid;
8. Propagation through the layer solid-liquid;
9. Refocusing to excitation source.



We assume that water and steel have the same physical properties that we discussed earlier and the difference is only in mechanical structure layout presented in Fig. 10.

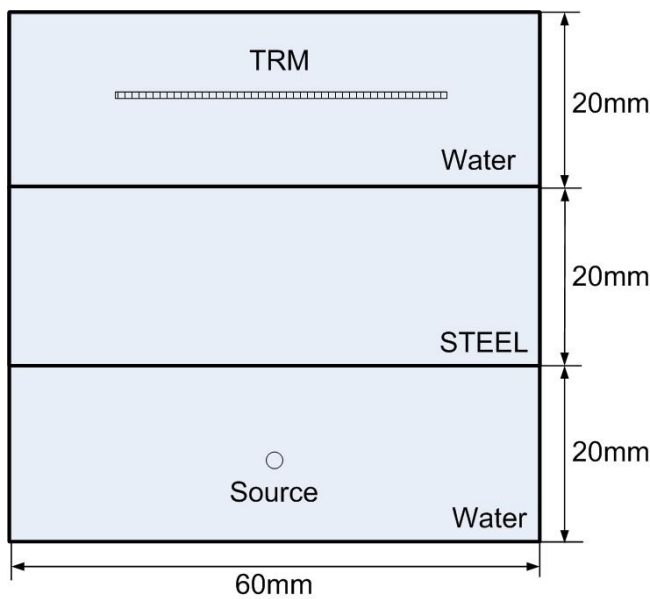


Fig.10. Geometrical layered structure setup

Modeling results

As in the previous section, we start with the forward wave propagation. The excitation source is a point pressure load applied to water at the position shown at the time $t = 1.84 \mu\text{s}$ with the coordinates $(x = 30 \text{ mm}, y = 10 \text{ mm})$. In the water we observe only the pressure wave and its wavefront. In the snapshot at $t = 3.4 \mu\text{s}$ we observe the transmitted and the reflected waves. At the time instant $t = 4.4 \mu\text{s}$ we can see shear waves (slower motion) traveling in the steel plate and pressure waves propagating through steel-water interface. The last snapshot ($t = 4.4 \mu\text{s}$) demonstrate a clear pressure wave, that was captured by the TRM which is located at the position $(y = 10, x\text{-centered})$ and recorded.

After the time-reversal operation $u(T-t)$ and transmission of the reversed wave pulses by the TRM we can observe back-propagated wavefield. At the time $t = 3.24 \mu\text{s}$ we can see that the wavefront of the back-propagated wavefield is similar to the forward-propagated, but the wavefront has a symmetrical wavefront in the opposite direction. After the fluid-solid interface we can see that many reflected waves disappeared and through the steel plate propagated “clean” pulsed wave (time $t=4.24 \mu\text{s}$

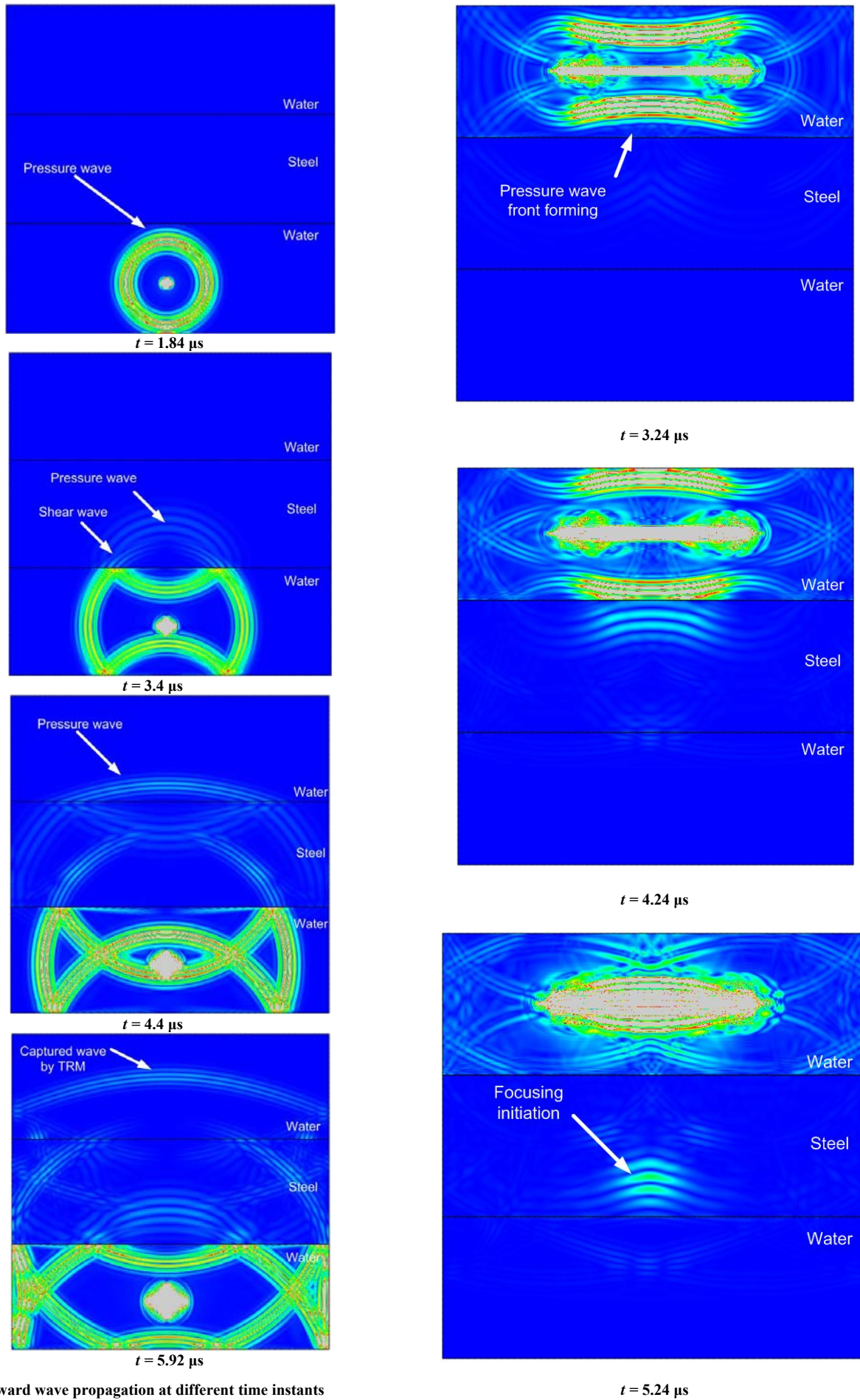


Fig. 11. Forward wave propagation at different time instants

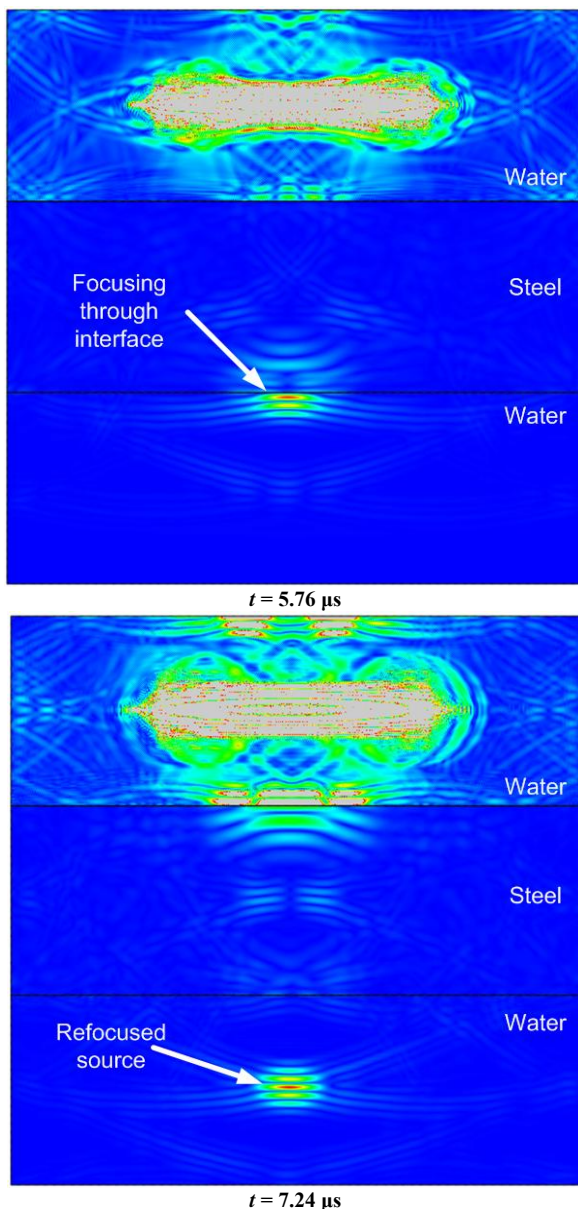


Fig. 12. Back-propagated time-reversed wavefield at different time instants.

and $t = 5.24 \mu\text{s}$). After the last solid-liquid interface, the traveling wavefield become more tight and at the time instant $t = 7.24 \mu\text{s}$ the amplitude achieve its maximum and it can be named as a refocused wave at its source.

The lateral resolution differs from the expression (6) because a new layer has been added and can be expressed as [5]:

$$l = \frac{\lambda_{PF}L_F + \lambda_{PS}L_S + \lambda_{PF}L_F}{d} . \quad (7)$$

Conclusions

In this article was investigated an application of the ultrasonic time-reversal approach to detection and characterization scatterers (defects) in multilayered plates. The results of the last section the snapshot at the time

$t = 7.24 \mu\text{s}$, Fig.12 illustrate that multiple reflections caused by different structure layers and boundaries were eliminated by the TRM. That property of TRM allows affirm an conclusion that the time reversal mirror can be successfully used in multilayered structures. Wave energy does not dissipate after mode conversion when the wave propagate through a liquid-solid interface, but is redirected to waves which are added in some arbitrary time instant.

References

1. **Fink M.** Time reversal of ultrasonic fields – Part I: Basic principles. IEEE Transactions on Ultrasonic, Ferroelectrics and Frequency control. 1992. Vol. 39. P. 555-566.
2. **Ing R. K., Fink M.** Time-reversed Lamb waves. IEEE Transactions on Ultrasonics, Ferroelectrics and Frequency control. 1998. Vol. 45. P. 1032-1043.
3. **Fink M.** Time-reversed acoustic. Scientific American. November 1999. Vol. 281. P. 91-97.
4. **Fink M.** Acoustic Time-Reversal Mirrors. Springer-Verlag, Berlin Heidelberg. 2002.
5. **Prada C., Manneville S., Spoliansky D., Fink M.** Decomposition of the time reversal operator: Detection and selective focusing n two scatterers. Journal of Acoustic Society Am. Vol. 99. P. 2067-3076.
6. **Borcea L., Papanicolaou G., Tsogka C.** A resolution study for imaging and time reversal in random media. Contemporary Mathematics. 2006.
7. **Blomgren P., Papanicolaou G., and Zhao H.** Super-resolution in Time-Reversal Acoustic. J. Acoust. Soc. Am. 2002. Vol. 111. P. 230-248.
8. **Prada C., Fink M.** Eigenmodes of the time reversal operator: A solution to selective focusing in multiple target media. Wave motion. 1994. P.151-163.
9. **Nunes I., Negreira C.** Efficiency parameters in time reversal acoustic: Application to dispersive media and multimode wave propagation.
10. **Barauskas R., Daniulaitis V.** Simulation of ultrasonic pulse propagation in solids. CMM-2003 – Computer Methods in Mechanics, Gliwice, Poland. 2003.
11. **Abaqus/Explicit™.** v6.3 Theory Manual sec. 3.1.1. 2005.
12. **Fouque J. P., Garnier J., Papanicolaou G., Solna K.** Wave propagation and time reversal in randomly layered media. Springer-Science, New York. 2007.
13. **Papanicolaou G., Tsogka C.** Time reversal through a solid-liquid interface and super resolution. Report. October 2002.

G. Butėnas, R. Kažys

Laikė apgręžtų ultragarso bangų fokusavimas daugiasluoksnišė struktūrose

Reziumė

Ultragarso bangų laikė apgręžos (*time-reversal*) metodo daugiasluoksnių struktūrų defektų lokalizavimui bei jų parametrms rasti teoriniai tyrimai atlikti pasitelkus baigtinių elementų programinį paketą *Abqus-EzPLICIT*. Tyrimų rezultatai parodė, kad laikė apgręžos metodu galima ultragarasą atrankiai fokusuoti į kiekvieną daugiasluoksnišės struktūros sluoksni ir į skirtinguose sluoksniuose esančius defektus. Taip pat parodyta, kad laikė apgręžto signalo energija, bangai sklindant per skirtingų sluoksnių ribas, neišsibarsto, bet dėsnigai išsiskirsto ir tam tikru laiku susitelkia į šaltinio vietą.

Pateikta spaudai 2008 06 25